

Chip-to-chip Communication by Optical Routing Inside a Thin Glass Substrate

Lars Brusberg, Norbert Schleppe, Henning Schröder
Fraunhofer Institute for Reliability and Microintegration,
Gustav-Meyer-Allee 25, 13355 Berlin/Germany,
lars.brusberg@izm.fraunhofer.de

Abstract

Most optical waveguide technologies on board level are using polymer materials. The drawback for these approaches are issues with post packaging processes because of thermal instabilities under thermal load, high optical loss in the infrared wavelength range and process challenges in case of single mode waveguide geometries.

A planar gradient index glass waveguide, optical mirror and refractive optic integration technology on wafer level will be presented here. 3D optical interconnects result inside a commercial available thin glass sheet. The waveguides are single mode and processed by a two step thermal ion-exchange technology. The propagation loss at 1310 nm is 0.2 dB/cm. The waveguides characterize a symmetric gradient index profile. Low coupling loss results between the waveguide and single mode optical fibers as well as optoelectronic components because of excellent mode matching. Different refractive optics are implemented by a field-assisted ion-exchange technology. An optical mirror is processed by laser ablation technology. The integration of waveguides, lenses and mirrors into an optical material like thin glass benefits of very high integration density and reliability. Processing thin glass by wafer level techniques in a planar way makes it compatible with post processes (e.g. thin film and assembling processes). In this approach thin glass is the platform for photonic integrated circuits, VCSELs and photodetectors. Thus flip-chip mounted photonic devices become optically interconnected directly by 3D optical pathways inside the thin glass substrate.

For this approach different building blocks and interfaces in between are designed and proofed by optical simulations. Building blocks are VCSEL waveguide coupling, waveguide detector interface, beam collimation for interposer board interface and PIC waveguide coupling. The concept is verified by experimental results. The glass based packaging concept, the design of each building block and the technologies for waveguide, mirror and lens integration are presented in this paper.

Introduction

The telecom wide area network is all single mode optical fiber based because of low dispersion and low loss in the wavelength ranges of 1310nm and 1550nm. In contrast local area networks having interconnection length typically shorter than 300m using multi-mode fiber interconnect. Multi-mode applications allow higher coupling tolerances that reduce the packaging costs that are quite high for photonic devices. Photonic packaging is challenging because of combining thermal, electrical and optical design, process and reliability requirements. An optical interconnection will replace an electrical one if performance is getting much higher or costs

decrease for manufacturing and operating. Replacing of high-speed electrical by optical interconnects on board level as well as on module level is just a question of time as a result of continuing rise in demand for bandwidth-hungry applications like video conferencing, high-definition television, video instant messaging or cloud storage.

In the near future, optical system interconnects on board and module level will be multi-mode and transceiver units like active interposers will be close to the electrical working computing unit. A much more advanced development as forced of Intel Corp. involves optical computing where the processor will have optical interconnects for inter-chip communication [1]. The technology behind that scenario is silicon photonics that is also used by Luxtera Inc. for AOC [2]. Using CMOS processing photonic integrated circuits with hybrid sources, photo-detectors, modulators, and wavelength multiplexers are integrated in the same chip as the processor core units called photonic integrated circuits (PIC). Silicon is transparent and well suited as waveguide in the wavelength range above 1107nm. Because of the high-index contrast between the silicon waveguide core and silicon dioxide cladding layer, the single-mode waveguide dimensions are on a nanometer scale. The high-index contrast allows very high integration densities but light coupling between a single-mode fiber and such a waveguide is challenging. Besides PICs, flip-chip bondable photonic components like VCSELs and photo-detectors are more and more available operating in the telecom wavelength range. For terabit computing and communication PICs supporting wavelength division multiplex (WDM) for Chip-to-chip communication using integrated waveguides inside a printed circuit board or interconnected by an optical fiber will getting necessary. The need for a packaging technology based on single-mode interconnects in the telecom wavelength range supporting chip-to-chip communication as well as telecom fiber interconnection increases.

Solving the interconnection and packaging problem we have developed a glass based photonic packaging approach called *glassPack* with integrated single-mode waveguides combined with electrical functionalities. Beyond that glass based packaging provides optical chip-to-chip interconnects in a package. The first part of the paper will present packaging concept for assembling of photonic components and fiber coupling on board-level and module-level, respectively, as well as the design for waveguides and lenses for optical routing inside the glass substrate. In the second part of the paper lens and mirror technologies are evaluated and experimental results are presented.

Packaging Concept

Thin glass as a substrate material has many benefits compared to conventional packaging materials like silicon,

ceramic or polymer based laminates because of its excellent dielectric and transparent properties that are becoming important for electrical high-frequency signal wiring as well as for optical waveguiding. Furthermore, the integration potential of glass is superior because of the dimensional stability under thermal load and the coefficient of thermal expansion (CTE) matching that of silicon ICs. Thus a small pitch size of conductor traces, small scale through-vias and high alignment accuracy are the key requirements that will be achieved from glass based packaging. The transparency of glass allows the planar integration of optical elements. A review of glass based packaging, requirements, suitable glasses is given in [3].

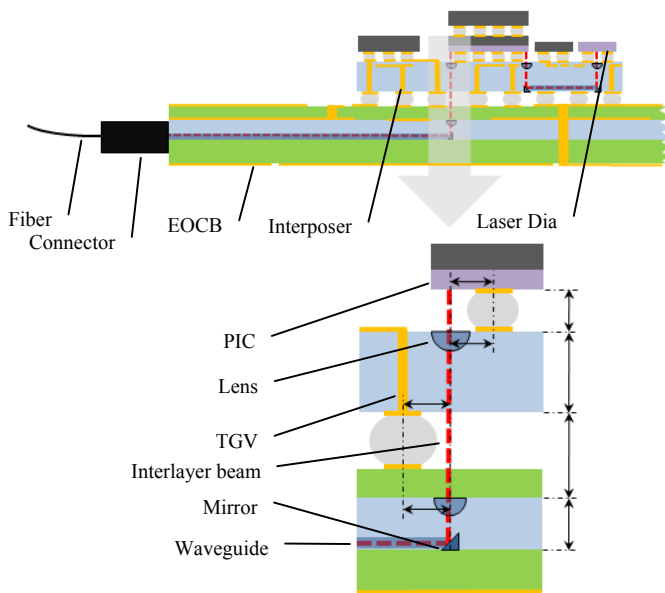


Figure 1. *glassPack* based integration concept: electro-optical PCB including electro-optical transceiver located close to processor unit

The envisioned glass based packaging approach for optical chip-to-chip communication is based on optical interconnects using single-mode waveguides for in plane (2D) and free space propagation for out of plane (3D) routing in a package. Thin glass is the preferred substrate material and integration of waveguides, lenses and mirrors is part of the concept for guiding the optical beam through the package. The outer world will be interconnected by single-mode optical fibers. To be compatible with silicon photonic PICs and telecom fiber networks the system is designed to be operated in single-mode at wavelength of 1310nm/1550nm. Thin glass with the integrated optical elements will be used as substrate for TGV interposers or embedded core layers in the electrical-optical circuit board (EOCB) as shown in Figure 1. The illustrated package consists of a through-glass-via (TGV) interposer with electrical and optical interconnects that is mounted on an EOCB having a glass core with integrated optical waveguides as well. Besides active and passive electrical components, photonic components are also integrated on the same substrate. The red lines present the optical paths passing lenses, mirrors and waveguides. The concept was already

proofed on a multi-mode based demonstration for the interposer [4] as well as for the EOCB [5].

The single-mode waveguide as well as the out of plane coupling considerations are enhancing the *glassPack* investigations generating generic module and board-based solutions for intra and inter-package optical highspeed communication.

Optical System Design

A design study of potential optical interconnect scenarios within the *glassPack* concept is presented in this section as a basis for selecting suitable process technologies for waveguide, lens and mirror fabrication. Technology results can be evaluated on matching to the performed optical design. So far nine building blocks define the potential interconnections within the packaging concept. Of course there are more optical interconnect scenarios of lower relevance that will not be considered at the moment for keeping focused. The first building block involves all 2D waveguide circuit elements like straight waveguides, bends, splitters and crosses. The coupling by an optical glass fiber in and out of the package is described as the second and third building block. The fourth building block covers the waveguide out of plane coupling for interlayer beam connection. To be compatible with further building blocks that interlayer beam is defined allowing higher coupling tolerances based on a collimated beam as depicted in Figure 1. All further building blocks are defining coupling of light between the waveguide or the interlayer beam and a photonic component can be a laser, detector or PIC.

The free space propagation vertical to the waveguide plane is implemented in a ZEMAX™ optical simulation. ZEMAX handles both sequential and non-sequential ray-tracing and in addition physical optics propagation (POP) in sequential mode. The non-sequential mode is used to model complex three-dimensional systems such as arrays of dies and for interlacing of different objects as it is required for modeling graded lenses or waveguides. Whereas the setup is optimized in sequential mode by means of physical optics to evaluate diffracting influences and in particular coupling efficiencies. The system efficiency Σ with the source amplitude function $F_s(r)$ and the amplitude transmission function of the optics $t(r)$ is one of the main criteria for evaluation the performance of the model. The second merit is the receiver efficiency Λ , including the receiving complex amplitude $F_r(r)$ and the wavefront amplitude from the exit pupil of the optical system $W(r)$. Highest coupling efficiency $\Xi = \Sigma \cdot \Lambda$ is achieved if the incident wavefront matches the mode profile at every point in both amplitude and phase.

An adequate system design is as important as a good receiver efficiency to maintain a high overall performance. This will in particular call for a balanced lens aperture to involve sufficient light in the optimization. Generally, the more powerful physical optics tool is applied to optimize each optical element and to define subsequent relevant design parameters such as lens apertures and curvatures.

The lowest-order mode for Laguerre-Gaussian beams yields to a circularly symmetric solution. Therefore, all optical single-mode sources in the simulations, be it a VCSEL

diode, a single-mode waveguide, a single-mode optical fiber or a collimated beam, will emit Gaussian beams into the model systems. Another welcome fact is that a Gaussian beam will remain Gaussian when transmitted through a set of circularly symmetric optical components aligned with the beam axis, as long as just the paraxial nature of the beam is maintained. In this case it is sufficient to consider beam width and wavefront curvature along the optical path.

For performing the simulations we specified parameters that are representing state-of-the-art system requirements as well as fitting to the packaging concept. For specifying component parameters, datasheets of commercial available devices were used. Because of the excellent properties as well as the compatibility of the waveguide process we used SCHOTT D263Teco™ glass as a substrate material. Thin glass sheets are available starting at a thickness of 30μm but are difficult to handle during processing. 500μm glass thickness is chosen that is commonly used in wafer-level packaging (WLP) and allows an appropriate distance for reducing beam divergence for coupling into the very low index contrast waveguides. Below, the design study for chosen building blocks are presented involving the setup, specified parameters and results for technology development and evaluation.

Building Block #1 Waveguide Circuit

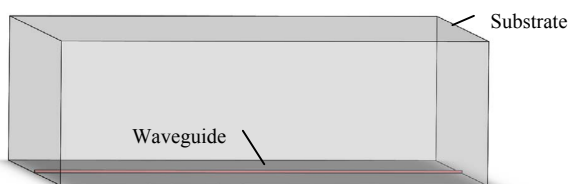


Figure 2. Schematic of building block #1

Already a single-mode waveguide technology based on a two step thermal ion-exchange has been developed using the commercial available thin glass sheet SCHOTT D263Teco [7].

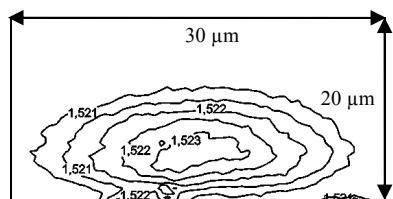


Figure 3. Single-mode waveguide refractive index profile (678 nm)

Similar to the straight waveguide process, all kind of waveguide elements can be processed by transferring the CAD layout to the thin film aluminum mask deposited on the glass substrate surface before the ion-exchange takes place through the mask openings. Basic waveguide elements are straights, bends, crosses and couplers that are part for waveguide devices like Mach-Zehnder Interferometer, ring resonators, star couplers or waveguide routing circuits. Waveguides with low mode confinement cause larger footprint of devices or circuits because of increased bend radius. The refractive index profile as shown in Figure 3

having a maximum index modulation of 0.003 indicates the very low mode confinement causes larger footprint of devices or circuits because of increased bend radius. Because of the elliptical waveguide profile the mode field diameter (MFD) is 13μm in vertical and 20μm in horizontal direction.

Building Block #2 Fiber → Waveguide

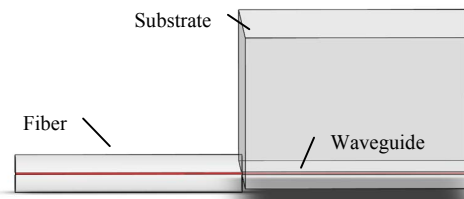


Figure 4. Schematic of building block #2

For coupling light from an optical fiber in plane to the waveguide circuit as shown in Figure 4, the fiber has to be positioned in front of the substrate end face. Goal is a high coupling efficiency. Loss of light is caused by:

- Poor end face preparation (extrinsic)
- Reflection losses (extrinsic)
- Separation distance (extrinsic)
- Lateral and angular misalignment (extrinsic)
- Core diameter mismatch (intrinsic)
- Numerical aperture mismatch (intrinsic)
- Refractive index profile difference (intrinsic)

For our investigations we are using Corning SMF-28e+ optical fibers. The key characteristics are summarized in Table 1.

Table 1. Specification for building block #2

Building Block Element	Specified Parameter		
Fiber	MFD	μm	10.4
	NA		0.09
	n (1550nm)		1.444
Waveguide	NA		0.09
	n (1550nm)		1.51

Intrinsic coupling losses are caused by mismatch between optical fiber and waveguide parameters. Extrinsic losses occur as result of the jointing technology. For confinement between elliptical waveguide mode and circular fiber mode the loss can be calculated using Equation 4.122 in [8]. In case, ellipticity is up to 15 % the loss remains smaller than 0.1 dB. Little mismatch in numerical aperture (NA) and refractive index are of much lower significance.

Building Block #3 Waveguide → Fiber

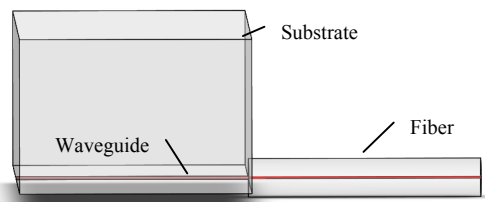


Figure 5. Schematic of building block #3

The reversed case of the previous building block presents the coupling of light coming out of the waveguide and into the optical fiber as shown in Figure 5.

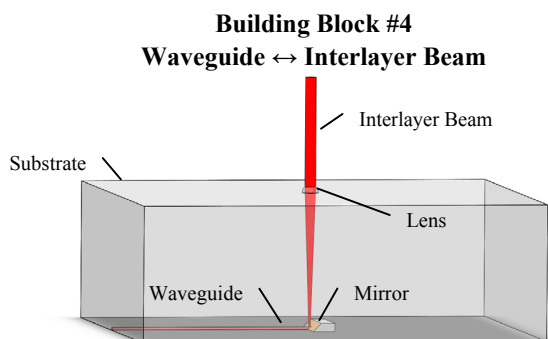


Figure 6. Schematic of building block #4

A further specification was made considering the lens integration part of the concept. Only one lens has to be used for keeping the optical system simple and controlling the lens technology later directly on the imaging properties by compromises in optical performance. In this building block, it may be desirable to collect an incident collimated beam (interlayer beam) and couple it into a SM fiber positioned vertically onto the thin glass or into a single-mode waveguide lying under the glass surface as shown in Figure 6. Both cases require adequate mode-field overlaps and can be resembled from this design study. Due to the immanent analogies only the coupling fiber is modeled. The light is focused already on its entry in the glass and coupled on the rear surface. Setting a suitable lens aperture is a first qualitative decision. While the diameter should be wide to collect as much light as possible, a bigger aperture will make manufacturing more challenging: the contact pads of the applied dies will limit the diameter of the element and economic processing times will prefer a smaller maximum sag. For these reasons the aperture diameter is set to be $60\mu\text{m}$.

Table 2. Specification for building block #4

Building Block Element	Specified Parameter		
Interface	Distance Range	mm	0...1
	MFD ($1/e^2$)	μm	50
Substrate	Glass Thickness	μm	500
	n (1550nm)		1.507
Mirror	Angle	deg	45
Waveguide/Fiber	MFD ($1/e^2$)	μm	9
	NA		0.09

The lens aperture diameter is chosen to be $60\mu\text{m}$ in order to maintain constant framework conditions to the following building blocks. Simulation parameters are summarized in Table 2.

A lens with $R = 170\mu\text{m}$ and $K = -1.31$ leads to a system efficiency $S = 81\%$ and receiver efficiency $T = 83\%$, which results in an overall coupling efficiency of $E = 67\%$ (Figure 7).

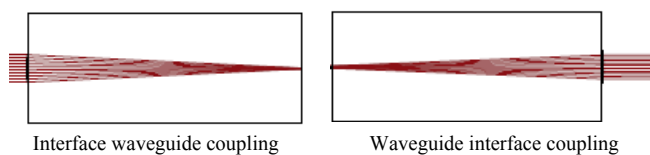


Figure 7. ZEMAX results of building block #4

The path of light in this case is bidirectional, so for the reverse design where the light of a single-mode fiber is collimated at the back surface on its exit, the same lens characteristics and lens parameters apply. The light from the waveguide/fiber has a beam diameter of about $64\mu\text{m}$ due to the fiber/waveguide NA and a divergence of 1.2° .

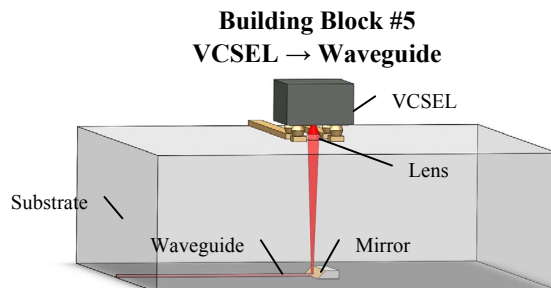


Figure 8. Schematic of building block #5

In this building block, as shown in Figure 8, a single-mode VCSEL emitting at 1550nm is assumed to be located $50\mu\text{m}$ above the upper glass surface. The distance lies within practical boundaries and ITRS [6] expectations. Curved surface lenses that are embedded in the glass are chosen for their high numerical aperture. As a result, the distance from lens center to the back surface of the glass substrate is $500\mu\text{m}$ as specified with all other simulation parameters in Table 3.

Table 3. Specification for building block #5

Building Block Element	Specified Parameter		
Laser	Divergence	deg	22.8
	(full angle; $1/e^2$)		
Substrate	Distance	μm	50
	Thickness	μm	500
	n (1550nm)		1.507
Mirror	Angle	deg	45
Waveguide/Fiber	MFD (v; h)	μm	9
	NA		0.09

The physical optics propagation (POP) result with the predefined settings yields to a lens radius $R = 22\mu\text{m}$ and a conic constant $K = -2.04$, whereas the maximum lens sag is found to be $15\mu\text{m}$. The simulation in Figure 11 gives a system efficiency $\Sigma = 100\%$, a receiver efficiency $\Lambda = 37\%$ and hence an overall coupling efficiency $\Xi = 37\%$. In comparison, the coupling efficiency without lens is $\Xi = 1\%$ and a ball lens with $50\mu\text{m}$ diameter yields to $\Xi = 2.5\%$. Moreover, a non-sequential modeling shows no optical cross-talk between two adjoining channels. The non-sequential optimization calculates with a channel pitch of $250\mu\text{m}$ and one million light rays.



Figure 9. ZEMAX result of building block #5

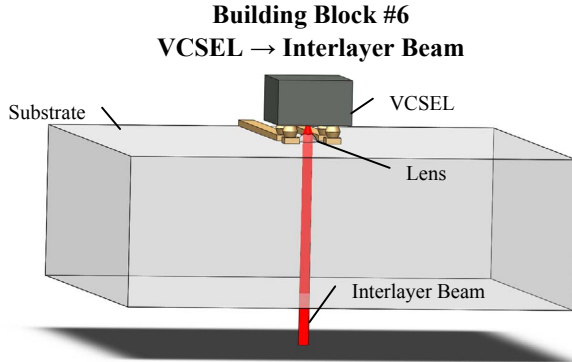


Figure 10. Schematic of building block #6

For optical interlayer connections, a collimated output beam is desired for flexible transmission distances. In particular, the light coming from laser diodes on top of the interposer is to be passed down to the glass embedded EOCB layer or further as depicted in Figure 10. In order to limit the collimated beam size, the diverging Gaussian is collimated on the top surface near the VCSEL diodes. Hence, the beam diameter will depend on the gap distance between laser die and glass substrate. As the distance remains to be 50 μm , the same lens diameter can be applied.

Table 4. Specification for building block #6

Building Block Element	Specified Parameter		
Laser	Divergence (full angle; $1/e^2$)	deg	22.8
	Distance	μm	50
Substrate	Glass Thickness	μm	500
	n (1550nm)		1.507
Interface	Distance range	μm	100
	MFD ($1/e^2$)	μm	38

Based on the specifications in Table 4, an optimization for the paraxial beam divergence at the exit of the substrate gives a divergence of 0.045 $^\circ$ for the Gaussian and a diameter of 38 μm . An investigation of the beam directly behind the lens shows a divergence of 0.031 $^\circ$ and displays the wave nature of the beam. Optimized lens parameters as result of the simulation (Figure 11) are $R = 27\ \mu\text{m}$ and $K = -2.34$. Maximum lens sag is 13 μm .



Figure 11. ZEMAX result of building block #6

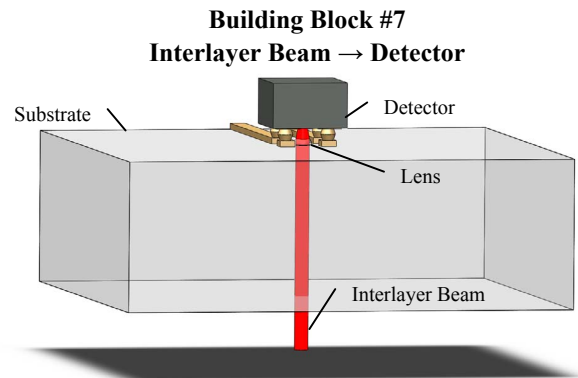


Figure 12. Schematic of building block #7

The thickness of the glass is rather irrelevant for the beam profile that is the next case in this design study and will be delivered by an incident interlayer beam that has to be focused on the active area of a photodetector as shown in figure 12. In analogy to the previous design study and the case for a fiber-to-interlayer beam, the incoming beam has a diameter of 50 μm and a divergence of 1.2 $^\circ$. The detector has an active area with 20 μm diameter, the distance between interposer and detector is 50 μm as specified in Table 5.

Table 5. Specification for building block #7

Building Block Element	Specified Parameter		
Interface	Distance Range	μm	100
	Diameter ($1/e^2$)	μm	50
Substrate	Glass Thickness	μm	500
	n (1550nm)		1.507
Detector	Diameter Active Area	μm	20
	Distance	μm	50

The prerequisites are limited and a 99% energy detection can be achieved by the simulation in Figure 15. In addition, main attention is turned on wave front optimization, which explains the strong conic $K = -132.65$ of the microlens besides $R = 23\ \mu\text{m}$. The beam profile on the detector surface is far from a Gaussian distribution due to typical nearfield behavior behind the lens.

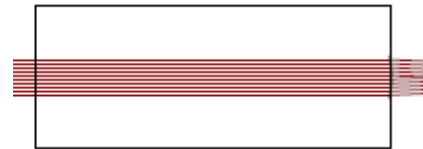


Figure 13. ZEMAX result of building block #7

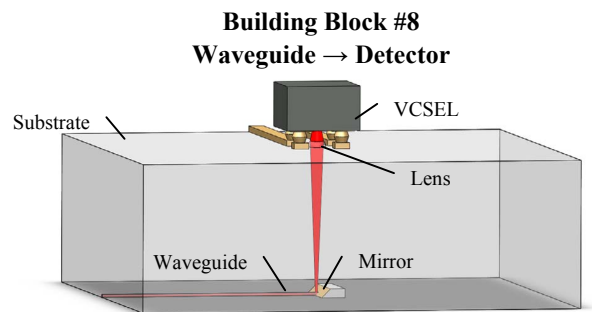


Figure 14. Schematic of building block #8

Instead of an interlayer beam, the output mode-field of a single-mode fiber or waveguide, respectively, at the lower surface of the thin glass can be imagined as shown in figure 14. The output profile of the fiber is known and described by the mode-field diameter $10.4\mu\text{m}$ and the numerical aperture $\text{NA} = 0.09$ as defined with all other parameters in Table 6.

The signal is to be detected by a photodetector diode $50\mu\text{m}$ above the glass surface. The gap is filled with air again. Common detectors have active areas big enough to capture all light even without beam focusing. However, in order to advance the system concept, the lower bound of $20\mu\text{m}$ in diameter is sought. As the detected energy dropped to about 80%, a detector diameter of $30\mu\text{m}$ is introduced. Whether the smaller detector with less efficiency is required or not has to be decided accordingly.

Table 6. Specification for building block #8

Building Block Element	Specified Parameter		
Waveguide	MFD (v; h)	μm	17; 10
	NA		0.09
Mirror	Angle	deg	45
Substrate	Glass Thickness	μm	500
	n (1550nm)		1.507
Detector	Diam Active Area	μm	20..30
	Distance	μm	50

The simulation as shown in Figure 15 observed $R = 26\mu\text{m}$, $\text{sag} = 11\mu\text{m}$ and $K = -4.08$ as suitable lens parameters. The setup detects 99% of the incident photon energy. Non-sequential simulations with two optical channels with $250\mu\text{m}$ pitch show no optical cross-talk.

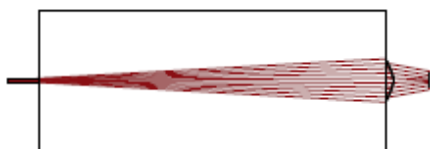


Figure 15. ZEMAX result of building block #8

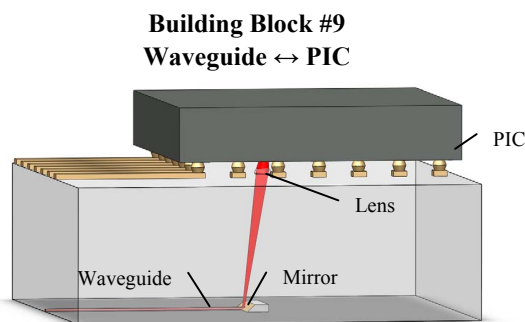


Figure 16. Schematic of building block #9

The optical simulations show good results for all evaluated design studies. In contrast to the previous design study based on specified parameters from device datasheets and ITRS forecasts, PIC devices are under research and data can be only extracted from scientific publications. A standard output profile of a PIC grating is not known so the design as shown in Figure 16 had to be postponed.

The simulation results furthermore showed that uniform lens characteristics such as lens position and lens aperture can be applied to all frameworks. Lens radius and conic that have to be adapted to each specific case lie in a close range so that a fabrication with one technology seems promising. However, since the lens sag is in the range of $10\mu\text{m}$, a deviation of the original distance of not more than 1% is expected.

Single-mode Waveguide Technology

Combining a suitable thin glass like SCHOTT D263Teco with the ion-exchange technology results in high-performing planar integrated waveguides that are highly compatible with standard packaging processes on board-level and wafer-level. The waveguide layout is defined by a mask pattern on the glass surface before the ion-exchange takes place. A structured aluminum mask deposited on the surface of the glass foil supports the locally confined diffusion process between the glass and the diluted silver salt melt. The small alkali ions in the glass are replaced by larger silver ions, which increase the refractive index in the glass. Then, a post process was performed by removing the mask pattern followed by a thermal ion-exchange in a pure sodium nitrate melt. Silver ions in glass diffuse back into the melt at the glass-melt interface or diffuse deeper into the glass. An elliptical and symmetrical index profile results with an index modulation of 0.003 as shown in Figure 3a. The index maximum is now buried from the surface into the glass. At a wavelength of 1550nm, the waveguide core has an index of 1.51 and a depth of $5\mu\text{m}$ below the glass surface. The insertion loss of a 90 mm waveguide sample is 2 dB. The process in detail as well as design and characterization of basic circuit elements like crosses, bends and splitters are presented in [7]. Waveguide technology will be further investigated for improved mode confinement to optical fiber modes and coupling efficiency.

Mirror Technology

Waveguide out of plane coupling is a requirement for 3D optical routing inside a thin glass substrate. An optical mirror integrated inside the glass positioned at the end of the waveguide deflects the light depending on the mirror angle. Mirrors have been already processed and the out of plane coupling was proofed having an attenuation of 1.33 dB at 1310nm [9]. The optical loss of deflection correlates with the mechanical surface quality and was not improved because the optical mirror is made of a 45 degree polished thin glass end face. The manufacture technology of the optical elements like a mirror has to be compatible at least with wafer-level, better with panel-level packaging. For these reasons we focused on mirror integration by V-groove laser ablation. A microscope picture of a laser structured mirror is shown in Figure 17. However, further investigations are necessary for mirror integration and in particular optical surface quality.

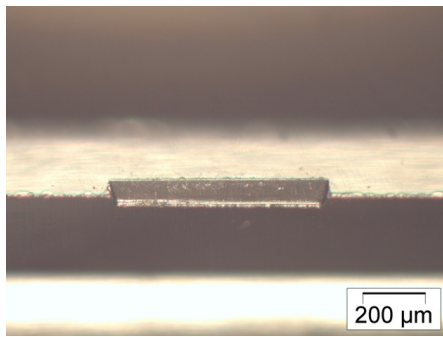


Figure 17. Microscope image of cross-section view of mirror element in thin glass substrate

MicroLens Technologies

An aspheric lens is one of the most powerful tools to shape the beam diameter within short distance. The goal is to place such a curved lens on the glass surface to enable direct photonic die placement above. Under these circumstances, the challenge is to integrate the lens into the substrate based on the lens parameters calculated by ZEMAX simulation as introduced above. So far, three potential lens technologies emerged that comply with the expectations and are furthermore combinable with existing manufacturing steps.

Ion-Exchange Fabricated: Microlenses are being buried within the substrate by means of an ion-exchange process, particularly under the presence of an external electric field. The possibility to maintain a plane glass surface along with the advantage of combining the fabrication of micro-optics with the implementation of gradient-index waveguides foster this investigation. The experimental results for the 2D run of the silver ion frontier of a cylindrical lens (Figure 18) and the refractive index increase $\Delta n=0.009$ (Figure 19) show reliable results that comply with expectations derived from the theory [6]. The surface swelling is suppressed successfully and the surface maintains good optical qualities ($R_a=0.001\mu\text{m}$). The experimental focal length of the lens depicted in Figure 19, verified by a subsequent ray-trace simulation, was found to be $(1513\pm 362)\mu\text{m}$ and does therefore not fulfill the requirements. Stacks of two and three planar microlenses in $300\mu\text{m}$ thin glasses show no significant improvement in the simulation. The ion-exchange technique is a good solution for implementing optical waveguides with low NA as shown in Figure 3, but the process fails for beam shaping on short lengths.

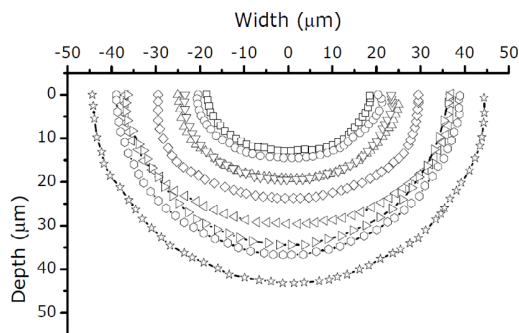


Figure 18. Run of the silver ion frontier ($300\mu\text{m}$ thin glass, $U=40\text{V}$, $T=275^\circ\text{C}$, process time: 10-90min in steps of 10min).

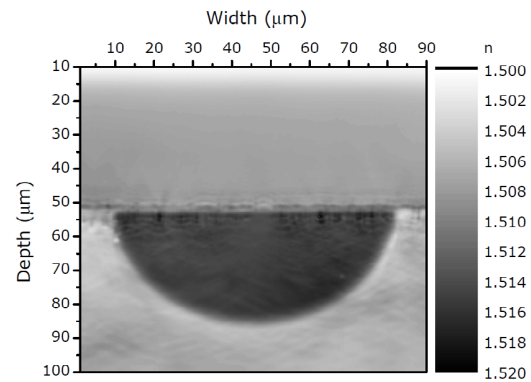


Figure 19. Refracted near-field image of a field-assisted ion-exchanged microlens ($300\mu\text{m}$ thin glass, process time: 70min).

Direct Laser Formed: The laser inherently is a fast and comprehensively usable tool that is already utilized for cutting and rounding glass substrates as well as implementing other optical elements, such as mirrors or prisms. Moreover, the fact that the introduced CO_2 laser will locally melt the glass ensures smooth surfaces with good optical properties ($R_a=0.001\text{mm}$). Lens arrays with $500\mu\text{m}$ and $250\mu\text{m}$ pitch are fabricated with irradiation time t from 0.2s to 2.0s and average irradiance P from 0.51W to 1.15W via pulse width modulation at 5kHz. While too small energies let the glass sag to form concave curvatures, high energies (around $t=2.0\text{s}/P=1.15\text{W}$) led to ablation. Figures 20 and 21 depict a working microlens with excellent circularity and overall lateral diameter of about $400\mu\text{m}$. Calculated focal length is $348\mu\text{m}$ in borosilicate glass. Biggest challenges are occurring strain and cracks due to thermal extension.

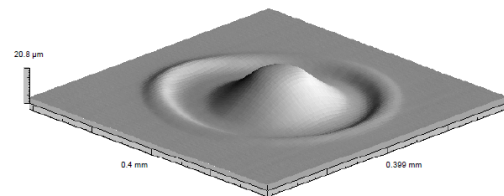


Figure 20. Direct laser-formed microlens (irradiation time t : 1s, irradiation intensity $P=1.15\text{W}$). Good circularity is given.

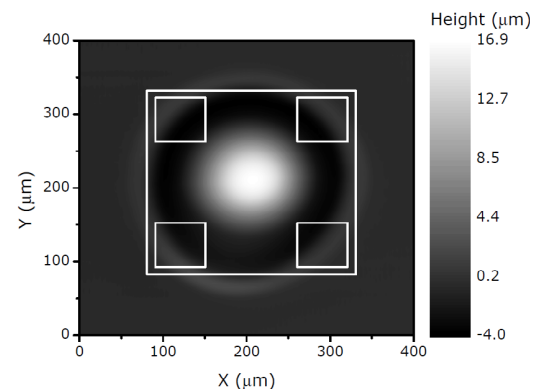


Figure 21. Top view of microlens from figure 21 with indicated die footprint ($250\text{mm} \times 250\text{mm}$).

RIE Fabricated: The third promising technology for microlens fabrication is an anisotropic reactive ion etching (RIE) process after thermal reflow of a photoresist mask. Preliminary etching samples on borosilicate glass showed good surface qualities ($R_a=0.001\mu\text{m}$) and lens pitches of down to $125\mu\text{m}$ are feasible. The etching ratio between glass substrate and photoresist is in the order of 1:6 so extremely thin, and yet round, etching masks are required. Further investigations on this field will follow.

Conclusions

Main focus was clearly the shaping of light during its passage through the glass substrate and efficient light coupling between distinguished optical components like waveguides and components like a VCSEL, detector or PIC. Within the framework of telecom systems, shaping light means in particular converging the signals from optical sources with inherited numerical aperture greater than zero to bundle the light on its free-running distances. The optical simulations show good results for the performed design studies. The simulation results furthermore showed that uniform lens characteristics such as lens position and lens aperture can be applied to all frameworks. Stacking several sheets is not necessary and one refractive element per design case is sufficient. The simulated performances are convincing, except for the coupling of a VCSEL into waveguide or fiber. Technologies for single-mode waveguides, optical mirrors and micro lenses have been presented. The waveguide process shows excellent results. Mirror and lens integration needs further investigations.

References

1. "Intel's Research in Silicon Photonics Could Bring High-Speed Optical Communication to Silicon", Intel White Paper (2004)
2. www.luxtera.com (2011)
3. Brusberg, L.; Schröder, H.; Töpfer, M.; Reichl, H.; "Photonic System-in-Package technologies using thin glass substrates," Proc. 11th Electronics Packaging Technology Conference, Singapore, pp.930-935 (2009)
4. Brusberg, L., Schröder, H., Erxleben, R., Ndip, I., Töpfer, M., Nissen, N., Reichl, H., "Glass Carrier Based Packaging Approach Demonstrated on a Parallel Optoelectronic Transceiver Module for PCB Assembling", Proc. 60th Electronic Components and Technology Conference, Las Vegas, NY, USA (2010)
5. Schröder, H. et al "Thin Glass Based Electrical-Optical Circuit Boards (EOCB) Using Ion-Exchange Technology for Graded-Index Multimode Waveguides" Proc. 59th Electronic Components and Technology Conf, Lake Buena Vista, FL, USA, pp. 268-275 (2008)
6. www.itrs.net/, ITRS roadmap update (2008)
7. Brusberg, L., Lang, G., Schröder, H. "Thin glass based packaging and photonic single-mode waveguide integration by ion-exchange technology on board and module level" Proc. of SPIE, Photonics West, San Francisco, CA, USA, No. 7944-11 (2011)
8. Voges, E., Petermann, K. "Optische Kommunikationstechnik", Springer (2002), ISBN: 3-540-67213-3
9. Schröder, H., Brusberg, L., Arndt-Staufenbiel, N., Tekin, T. "Out-of-Plane Coupling Using Thin Glass Based Arrayed Waveguide Components" Proc. SPIE Photonics West, OPTO, San Jose, CA, USA (2009)
10. Wakaki, M. *et al*, "Microlenses and Microlens Arrays Formed on a Glass Plate by Use of a CO₂ Laser", Appl. Opt., Vol. 37, No. 4, pp. 627-631 (1998)
11. Lilienhof, H.-J. *et al*, "Field-Induced Index Profiles of Multimode Ion-Exchanged Strip Waveguides", IEEE J. of Quantum Electronics, Vol. QE-18, No. 11, pp.1877-1883, (1982)